

Modelling Induction Heating of a solid round bar for a new 3D Metal Printer Method

Jack E. Alley¹

University of New South Wales at the Australian Defence Force Academy

Dr. Sean O'Byrne identified a new method to create three dimensional metal objects using three dimensional printing. This new method was thought of to design a three dimensional printer that would be energy efficient and affordable for the consumer market. This new method uses induction heating as the heating element in a fused deposition modeling three dimensional printing process. To be able to design such a three dimensional printer, a validated mathematical model is required to be able to calculate the rise in temperature in a tube from induction heating. To create and validate such a model the theory of induction heating is researched to calculate the heat generated in a round solid bar. Then the heat transfer equations were evaluated for the specific application. From this a MATLAB Model was written to calculate the rise in temperature in a round solid bar. An experiment was then conducted to validate the model. The experiment didn't provide accurate results however it showed that the model required additional work. This lead to a new model being written that agreed more with the behavior of the induction heating process in a round solid bar.

Contents

I.	Introduction	2
II.	Project Outline	3
	A. Motivation	3
	B. Aims	3
	C. Methodology	3
III.	Modelling Induction Heating in a Solid Bar	3
	A. How to calculate the heating rate in the Solid Bar	3
	B. Equations for magnetic flux	4
	C. Equations to find the voltage drop on the surface	4
	D. Equations to find the equivalent resistance and joule heating	4
	E. Equations to find skin depth and heat distribution in the solid bar	5
	F. Equations to find the temperature change after heat induction	5
IV.	Modelling Heat Transfer in a Solid Bar	5
V.	MATLAB Model	6
	A. Problems and Observations	6
	B. Results	7
VI.	Experiments	7
	A. First experiment	7
	B. Issues with results	8
	C. Final recorded results	9
VII.	Revised MATLAB Model	9
	A. Modifications	9
	B. Results	10
VIII.	Conclusions	11
IX.	Recommendations	11
	Acknowledgements	11
	References	11

¹ OFFCDT, School of Engineering & Information Technology. ZEIT4500/4501/4297 – delete as appropriate.

APPENDICES

Appendix A. Plot of experiment temperatures and the temperatures calculated using regression	A1
Appendix B. Plots of the temperature distributions in the bar every 50 seconds	A2

Nomenclature

α	= thermal diffusivity [m^2/s]
a	= diameter of the electrical reference path [m]
K_r	= the correction factor for resistance in the bar due to an alternating current [Ω]
A	= the reference area the electrons are passing to calculate resistance [m^2]
$I(t)$	= alternating current running through the coil [A]
I_A	= amplitude of the alternating current running through the coil [A]
ϕ_β	= magnetic flux [$T \cdot m^2$]
c_p	= specific heat coefficient [$J/kg \cdot K$]
B	= magnetic field strength [T]
δ	= skin depth [m]
f	= frequency [$1/s$]
l	= length of the coil [m]
i	= node position for the radius
j	= node position for along z axis
μ	= permeability [H/m]
μ_r	= relative permeability
μ_0	= permeability of free space [H/m]
V_{drop}	= potential drop on the surface of the bar [V]
N	= number of turns of the solenoid per unit length
π	= pi
P	= heat distribution in the bar [W]
H	= heat generation [W]
P_{surf}	= heat rate on the surface of the bar [W]
R_{surf}	= resistivity [Ω]
σ	= electrical conductivity of the bar [$(\Omega \cdot m)^{-1}$]
ρ	= electrical resistance of the bar [$\Omega \cdot m$]
k	= thermal conductivity of the bar [$W/m \cdot K$]
t	= time [s]
r	= radius cylindrical axis [m]
R_{max}	= radius of the surface of the bar [m]
ΔT_{gen}	= temperature difference due to heat generation [K]
v	= reference volume for the change in temperature by heat generation [m^3]
ρ_{bar}	= density of the bar [kg/m^3]
Δt	= change in time [s]
ΔT	= change in temperature at the node [K]
Δr	= distance between the nodes along the radius [m]
ϕ	= radial cylindrical axis [rad]
z	= axial cylindrical axis [m]
H	= heat generation [W/m^3]
Bi	= Biot number
FO	= Fourier number
E	= Emissivity

I. Introduction

Three dimensional (3D) printing has become a favorable fabrication technique that allows computer aided design (CAD) drawings to be produced as a tangible object. There are a large number of different printing techniques used to produce 3D objects. These can be made from a range of materials including plastics, metals and composites [1]. 3D printers have a large number of industrial and commercial applications and can be employed for many uses ranging from the one off production of a quick product prototype to a large scale printing of a complex engineering component. Future research may result in 3D printers becoming common household appliances, enabling users to purchase a product on the internet and then print them at home.

3D printing is becoming more popular however the commercial market still lacks an effective 3D printer for metals. Currently 3D printers for metals available to the wider public are highly energy inefficient and expensive. The production of a commercially viable technology for 3D metal printing would allow for the

creation of simple models and complex engineering components. There is potential for a high demand for a printer which can satisfy the needs of the commercial market.

Such a 3D printer design would use fused deposition modeling (FDM) process as it involves the direct depositing of the material used to create the object. Induction heating in the FDM process would be used as the heating element in the nozzle to melt the depositing metal. The nozzle design would involve a coil wrapped around a high curie temperature magnetic metal tube with a metal that has a lower melting temperature the curie temperature of the tube being deposited.

II. Project Outline

A. Motivation

The concept of a three dimensional printer using induction heating was conceived by Dr. Sean O'Byrne. It was found that a three dimensional metal printer using induction heating would be more efficient and effective than current designs. This would lead to designing a 3D metal printer for household consumption, where a person would be able to print items at home with the purchase of a CAD drawing.

R. McCormack started researching the idea, last year (2013), and produced a document that suggested that there potential to design a small scale, 3D printer for metal [2].

Continuing on from McCormack's research a program that models the rise in temperature in a tube is required. Having a validated mathematical model would allow for desired specifications to be simulated to determine whether or not it would perform effectively.

B. Aims

The aim of the project is to be able to produce a validated mathematical model of the induction heating process in the tube. The model would then be able to simulate, for a given set of inputs and parameters, the rise in temperature in a hollow cylindrical tube. This would determine if the inputs and parameters would meet the desired requirements. The main requirement to meet is being able to heat up the inner diameter of the tube to the melting temperature of the depositing material.

C. Methodology

To be able to create such a model first the theory of induction heating was researched so that the equations to calculate the heat generated were known. Next the heat transfer equations were researched and evaluated for the specific application. These equations were then used in a MATLAB Model to simulate heating up a solid round bar by induction. A solid round was simulated as it was simpler case to validate the model. Heating up a hollow cylindrical tube would be able to be simulated once the model was validated for the solid bar. Experiments were then conducted using an induction heater to heat up a solid round bar. The results of the experiment and the simulation were then compared. The model was then reconfigured and improved as necessary to more accurately meet the results of the experiment. This would validate whether or not the model can be used to simulate nozzle designs for the creation a 3D metal printer using induction heating.

III. Modelling Heating in a Solid Bar by Induction

A. How to calculate the heating rate and temperature change in the Solid Bar

Induction heating, heats the metal solid round bar inside the coil by a varying magnetic field caused from running an alternating current (AC) through the coil. The varying magnetic field induces eddy currents in the metal that change direction with the change in the field. Eddy currents are a closed electrical circular path that electrons follow in the metal. Every time the eddy currents change direction there is a potential drop because the electrons need to release energy to change direction. This release of energy is thermal energy which is heating up the solid bar [3].

To be able to calculate the heating rate generated by induction heating the magnetic flux first needs to be calculated. This is because the strength of the magnetic flux affects how big the potential drop is. Then the potential drop on the surface can be calculated. Only the voltage on the surface can be calculated as the magnetic field strength isn't uniform within the solid bar for a varying magnetic field as the electrons in the solid bar concentrate on the surface. This is due to the effect called skin effect. The distribution of heating in the solid bar can then be calculated from finding the skin depth and using joule heating equations. Once the distribution of heat is known within the bar the temperature change can be calculated for heat added for an amount of time.

B. Equations for the magnetic flux

The magnetic flux is affected by the magnetic field strength that is caused by the AC in the coil. The magnetic field strength is affected by the permeability of the metal the bar is made out of, the magnitude of the current and the number of turns per length of the coil. This can be shown by the formula for the magnetic field below [4, 3]:

$$B = \mu \frac{N}{l} I(t) \quad (1)$$

The relative permeability of the metal increases the strength of the magnetic field by increasing the density of the field. This is caused by the hysteresis effect in magnetic materials. Nonmagnetic materials will have a relative permeability close to one and so the magnetic field inside the coil would be the same as if nothing was inside. Magnetic materials have this affect due to the magnetic dipoles in the material wanting to align with the direction of the magnetic field. With a varying field they continuously change direction aligning themselves with the field which causes friction between the molecules adding more resistance and more heat generation. This affect has a limit as once the magnetic material reaches its curie temperature, which is below its melting temperature, the magnetic dipoles will no longer exhibit such a behavior.

The direction of current affects the direction of the magnetic field as the magnetic field lines are perpendicular to the flow of the current which can be seen using the right hand rule with the thumb in the direction of the current. The AC follows a sin wave and is shown by this equation [4]:

$$I(t) = I_A \sin(2\pi f t) \quad (2)$$

The magnetic flux is the magnetic field strength multiplied by the cross sectional area of the bar. This suggests that to increase the magnetic flux the area of the bar should be increased. This is true however impractical as the area of the coil needs to be greater than the bar so that the bar doesn't heat the coil and increasing the area of the bar would mean a greater mass would be required to be heated.

C. Equations to find the voltage drop on the surface

Faradays Law allows for the potential drop created by the change in direction of the eddy current to be calculated by [3, 4]:

$$V_{drop} = N \frac{d\phi_B}{dt} \quad (3)$$

This formula is only accurate for finding the potential drop of eddy currents on the surface as the distribution of electrons isn't uniform throughout the solid bar. Again it can be seen that by increasing the number of turns in the coil increases the magnitude of the potential drop. The potential drop can also be increased by increasing the frequency and the amplitude of the AC. The potential increases because a greater rate of change is created when the AC reverses direction.

D. Equations to find the equivalent resistance and joule heating

The AC changes the behavior of the resistance in the bar as the current density is greatest on the surface it has the greatest resistance. The formula for finding the resistance on the surface is [3]:

$$R = \rho \pi a K_r \frac{N^2}{A} \quad (4)$$

The formula is different from the resistance in a uniform current as it is affected by the number of turns in the coil (N) and a correction factor (K_r). The correction factor is for the non-uniform electrical path within the bar. This equation is used to calculate the resistance on the surface and the correction factor will be equal to 0.95 as the reference depth will be greater than 24 [3]. The reference is calculated by dividing the diameter being examined by the skin depth. The skin depth is defined later. It can be shown that by increasing the resistance by having more turns in the coil will decrease the amount of heat generated. This is because of joule heating equations shows that the heat rate is equal to [3]:

$$P_{surf} = \frac{V_{drop}^2}{R} \quad (5)$$

From this it's seen that increasing the potential drop and decreasing the resistance will increase the amount of heating generated in the bar at the surface.

As the heating rate is affected by the AC an average value for the magnitude of the potential drop will be used. The joule heating equations allows for the heat generated on the surface to be calculated.

E. Equations to find skin depth and heat distribution in the solid bar

Now that the heat rate on the surface can be calculated the distribution of heating throughout the bar can be found. The distribution of heating in the bar can be found using this formula [3]:

$$P = P_{surf} e^{(r-R_{max})^2/\delta} \quad (6)$$

The skin depth is when the heat rate is 14% that of the surface because of the skin effect. This effect is caused in conductors by the AC and is what causes the non-uniformity of the heat rate within the bar. The depth at which the heat rate is 14% of the surface can be found by [3]:

$$\delta = 1/\sqrt{\mu_r \mu_0 \pi f \sigma} \quad (7)$$

The formula shows that for higher frequencies and higher relative permeability materials the skin depth decreases. This means heating will be concentrated at the surface which would suggest that a smaller diameter bar would be easier to heat than a larger one not only due to the larger volume of the larger diameter bar but because of the penetration of the eddy currents.

F. Equations to find the temperature change after heat induction

Finally to calculate the temperature change from the amount of heat added to the bar can be found from the following formula [5]:

$$\Delta T_{gen} = P \Delta t / v \rho_{bar} C_p \quad (8)$$

The formula is derived from heat transfer equations when a volume of mass at an initial temperature has a constant heat flux added to the volume. It will raise the temperature after heat is added for an amount of time. This formula assumes uniform heat flux across the volume which isn't true however later it will be shown that that this won't matter when using finite differencing methods (FDE).

IV. Modelling Heat Transfer in a Solid Bar

To model the heat transfer in the bar, after heat has been added by induction, the general heat equation in cylindrical coordinates was evaluated. This equation is given below [5]:

$$\frac{\Delta T}{\Delta t} \frac{1}{\alpha} = \frac{\partial^2 T}{\partial r^2} + \frac{\partial T}{\partial r} \frac{1}{r} + \frac{\partial^2 T}{\partial z^2} + \frac{\partial^2 T}{\partial \phi^2} \frac{1}{r^2} + \frac{H}{kv} \quad (9)$$

This equation was then simplified to a one dimensional transient heat conduction equation in the radius direction. I assumed that the heat in the z and radial direction were uniform as there wouldn't be any change in heat due to uniform heating. The heat is added exponentially from the surface so the higher temperature on the surface would be cooled by the lower temperature in the center in the r direction. Heat radiation and heat convection were assumed to have no effect at the boundaries. Later it will be shown that H will be added first and then the transfer in heat will be calculated so heat generation in the equation has been taken out. The equation is then simplified to:

$$\frac{\Delta T}{\Delta t} \frac{1}{\alpha} = \frac{\partial^2 T}{\partial r^2} + \frac{\partial T}{\partial r} \frac{1}{r} \quad (10)$$

At first I tried to solve this equation by treating it as an ODE and solving it using a modified parametric Bessel equation. This proved to be too complicated to solve not only by hand but also in MATLAB. It was difficult to solve it because it relied on the boundary conditions to solve the equation and it was also difficult to write a Bessel equation in MATLAB.

I decided to then use explicit central finite differencing methods to find the change in temperature after heat is added and after heat conduction. This method doesn't use an exact calculation to solve the change in temperature. For a point along the radius it analyses the temperature before and after it and calculates the temperature change after a given time. This equation is shown below [6]:

$$\Delta T = \alpha \Delta t \left(r_{i+1} \left(\frac{T_{i+1,j} - T_{i,j}}{\Delta r} \right) - r_{i-1} \left(\frac{T_{i,j} - T_{i-1,j}}{\Delta r} \right) / r \Delta r \right) \quad (11)$$

To calculate the temperature change along the radius, it needs to be broken up evenly into nodes that can be individually analysed. The nodes on the boundary need ghost points to calculate the temperature change. As I had assumed that there were no losses I made the ghost points equal to the node being analysed.

The stability criterion wasn't identified until the MATLAB Model was first run but it will be explained here. Finite differencing will produce an unstable solution if the stability criterion isn't met. The criterion for this finite differencing method is met by the following rule:

$$\Delta t \leq \frac{\Delta r^2}{2\alpha} \quad (12)$$

This means that if the change in time for the calculated temperature change is greater than the right hand side a unstable solution will be produced. The unstable solution is presented by oscillations in the temperature distribution.

V. MATLAB Model

The model needs to be able to find the temperature distribution after heating the bar for a set amount of time. The inputs required for the model are the properties of the bar and the coil, the frequency and the amplitude of the current flowing in the coil and the spatial distance between the nodes. Also the total amount of time the bar is to be heated as this dictates when the model will stop. With those inputs the MATLAB Model calculates the temperature distribution after the specified amount of time by running a main script. Figure 1 is a block diagram showing how the model runs.

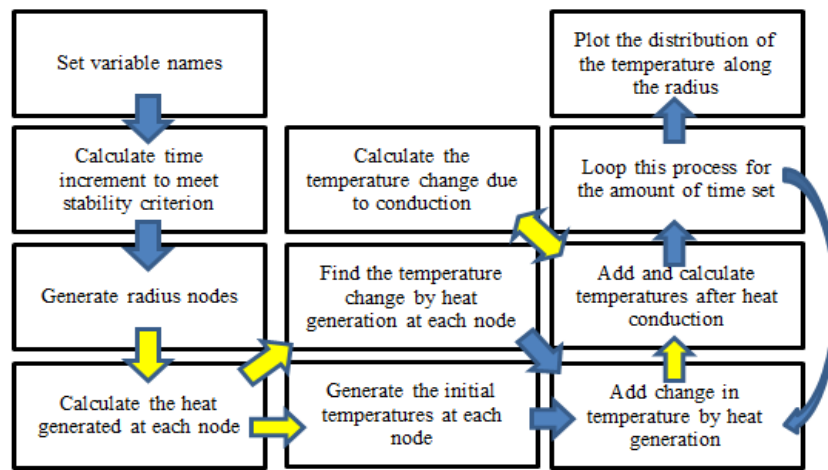


Figure 1. Block diagram outlining how the MATLAB Model works
Yellow arrows are called upon function and blue are steps in the main script.

A. Problems and Observations

As previously mentioned, the first problem occurred in the model was an unstable solution being produced. This was fixed by not setting the time increment at the start but instead calculating the maximum time increment that was allowed by the stability criterion.

After a stable solution was calculated two other problems noticed were the temperature change values were unrealistic for the time increment and the rise in temperature varied with the decrease in distance between nodes.

The problem with the unrealistic temperature rise was solved by evaluating the equations used to calculate the heat generated by induction. The equations used at first weren't correctly taking into account the direction of flow of the electrons in the bar. This affects the calculation for resistance as at first the length in the equation was assumed to be the length of the bar inside the coil but was actually the length of the path traveled by the electrons. The resistance value did affect the calculation of heat but unrealistic magnitudes of the temperature were still being produced.

The equations used at first were different to the equations used above. To find the heat generated the current on the surface was found by finding the current density on the surface instead of the potential drop. Then by finding the current density distribution, similar to how the power distribution was found, all that was required was the area the electrons were travelling through multiplied by the current density for that area gave the current flowing in that area. Using joules heating equations the heat rate could then be found for that radius node. The current density however was found by multiplying the electric field strength by the conductivity. This was found to be an incorrect method of finding the current density as this could only be used to calculate the current within the entire bar not just the surface. The formulas that are written above are the new and correct method to calculating the heat rate.

Accuracy of the model was then questioned when the distance between nodes was decreased. Decreasing the node spacing meant that the calculation of the central differencing had less of a truncation error. This error is in the order of magnitude of Δr^2 so by decreasing the distance between nodes decreases this error. What wasn't known was the limit at which the error was small enough to give the most accurate answer. The reason for this is because the more the distance is decreased the longer it takes the model to calculate the temperature distribution for the same heating time and the temperature distribution decreased as well. This was later looked at when the model was compared to the conducted experiment results as it was unknown when the value of Δr was small enough to give an accurate answer.

B. Results

Figure 2 is the plot of the results for heating the bar for 2 seconds with an input of 30A at 50000Hz.

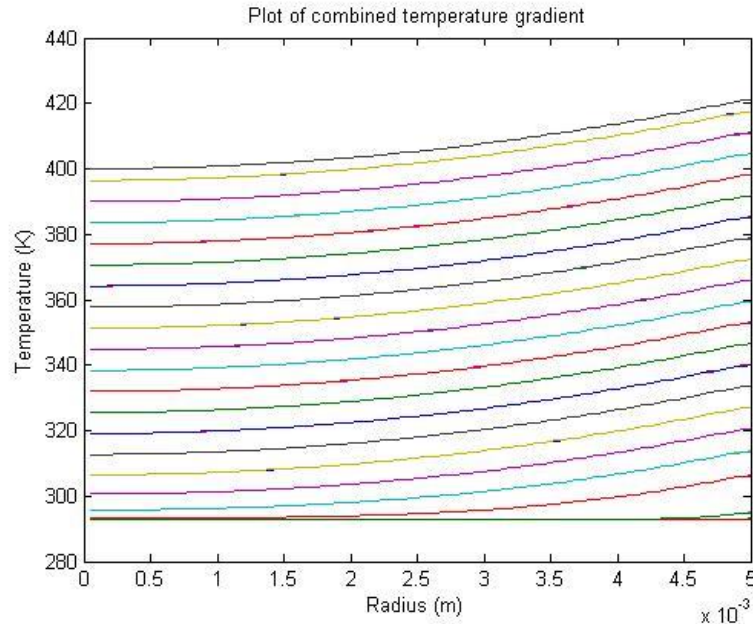


Figure 2. Plot of the temperature distribution in the bar at various

The colour of the lines don't represent temperature.

The results show the temperature distribution at the start and then the distribution after every 1000 time increments until the final temperature distribution when time is 2 seconds. It shows that the surface is the highest temperature and remains so whilst heating. This is because the most amount of heat is added to the surface. Heat conduction quickly transfers the heat to the center of the bar. It is then shown that as time continues the temperature gradient doesn't change.

VI. Experiments

The experiments involved heating a solid metal bar made out of mild steel that had a diameter approximately 5mm. To heat the bar, it was held vertically in a clamp inside a coil that was made out of litz wire. The coil was turned three times in 40mm with an inside diameter of 12mm. The AC was supplied by a ROY 1500 made by Fluxion that was able to vary the amount of power supplied to the coil. To measure the AC in the coil a Tecktronix TM502a power module with a clamp amp meter was connected to a GW INSTEK GDS-2064 oscilloscope. A multimeter was used to measure the voltage and the frequency of the AC in the coil. In some of the experiments a TAC80B-K Thermocouple made by OMEGA and a thermometer gun was used to measure the temperature on the outside of the bar. A MikroScan 7200V Thermal Imager was also used to measure the temperature on the surface of the bar.

A. First experiment

The first experiment was to determine the amount of current supplied to the coil. This only involved the multimeter to measure the current and the thermometer gun to measure the temperature on the outside of the bar as well as the coil.

The knob on the ROY that controls the amount of power supplied was adjusted from the lowest setting and then increased in half increments. It was able to get to the fourth increment before the ROY stopped due to an error. The error was caused because there was too much current running through the multimeter for it to handle. The multimeter was rated to 20A which suggests the fuse broke and a current higher than 20A was flowing in

the current. This stopped the ROY from working because to measure the AC the multimeter had to be connected in series with the coil.

The test was then started again without the multimeter to see how hot the bar could get. Not long after the power was adjusted past the fourth power setting the woolen insulation on the outside of the litz wire started to melt and the litz wire started to deform. This suggested that a thicker litz wire was required to carry the AC as the resistance within the wire heated it too much. Increasing the thickness of the wire allows for the current to flow through a larger area which decreases the amount of heat caused by the resistance in the wire.

B. Issues with results

After the first experiment the actual experiment that would be used to validate the MATLAB Model conducted. It involved using the thermal imager to record the temperature on the surface, using the multimeter to measure the voltage and frequency and the power module with a clamp amp meter connected to an oscilloscope to measure the current RMS. The thermal imager would provide a maximum temperature on the surface against time plot so that it could be compared against the model. The frequency and current was required so that the correct inputs were used in the model.

The current was never accurately measured after using the multimeter. This was because the clamp amp meter and the power module couldn't measure accurately the AC at a frequency that was higher than its specifications which was in the hundreds of Hz. The measurements of the current shown on the oscilloscope from the power module were compared against the multimeter for low power settings. This was to validate that the current readings weren't accurate. The multimeter had measured lower current RMS values than the oscilloscope and the difference increased with the increase in power setting. At this stage no other method of measuring the current was identified so it was continued to be measured using the power module, clamp amp meter and the oscilloscope.

There was also issues with measuring the max temperature on surface of the bar using the thermal imager. This was due to the thermal imager not being able to be calibrated correctly. To calibrate it the thermometer gun was used to measure the temperature on the surface of the bar with no heat applied and the camera then had its emissivity setting changed so that the temperature on the imager was the same as the gun. This worked for when the settings on the thermal imager were set for the lowest temperature range however the bar was able to be heated up to temperatures above this range. The thermal imager was then adjusted for the second temperature range of 0°C to 500°C. For the same emissivity reading a different temperature was given by the imager and the emissivity couldn't be adjusted to match the gun. A thermocouple was then used as a more accurate method of measuring the temperature on the surface of the bar but still the temperatures couldn't be match. The two didn't match for ambient temperatures so I decided to heat the bar up and then match the thermocouple with the imager while the bar cooled. The temperature from the thermocouple only could be read when the bar was cooled as when it was being heated the changing magnetic field affected the reading on the thermocouple. Now the thermocouple reading could be matched to the thermal imager except for only a certain temperature. Theory suggested that the emissivity value changes with increase in temperature however this was for very high temperatures. From theory an emissivity value was chosen and kept constant during the remainder of the experiments.

Another way to try and accurately measure the temperature involved recording the bar cooling with the thermocouple and then plotting the temperatures. Then by using regression a formula could be generated so that for an input temperature measured on the imager, a thermocouple temperature would be given as the thermocouple was said to be accurate. This would have worked except then the oscilloscope used to measure the thermocouple temperatures started showing irregular results where the temperature seemed to be oscillating, increasing and decreasing in temperature when the ROY was turned off. A formula was computed before this happened and it was identified that only the data recorded by the imager at the same time the data recorded by thermocouple could be used. This is because every time the thermal imager was turned off and it was recalibrated which gave different temperatures and so the formula would have to be recalculated. A plot showing the temperature recorded by the thermal imager on two separate days and the recalculated temperatures using the formula is shown in appendix A1. The plot shows that the temperatures recorded by the imager on the first day were greater than the thermocouple but on the second they were less.

C. Final recorded results

The last results recorded had the thermal imager set to an emissivity of 0.8 as this was found to be a realistic value of the emissivity [7]. Figure 3 shows the plot of the results.

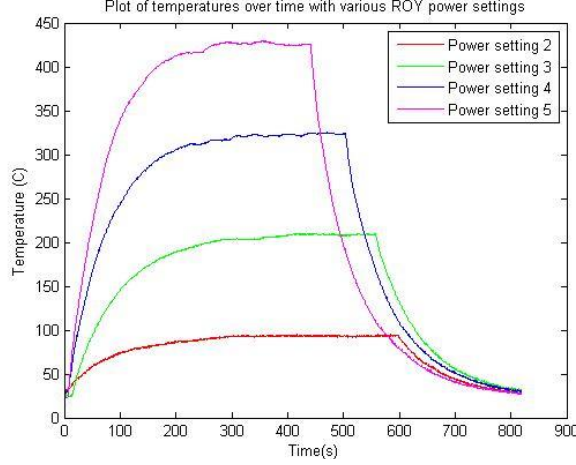


Figure 3. Plot of the maximum temperatures on the surface of the bar for various power settings

Though the plot of the measured temperatures versus time isn't accurate, it shows that the MATLAB Model wouldn't be validated. This is because the plot shows that eventually the losses and the heat generated by induction will equal and a constant maximum temperature for the set frequency and current will be reached. Therefore the assumption that losses at the boundary would have no affect was wrong and so the MATLAB Model needed to be changed to take into account losses so that it would exhibit a similar behavior. The MATLAB Model wouldn't however have to match the temperatures as the thermal imager results weren't accurate.

VII. Revised MATLAB Model

A. Modifications

It was identified that the heat transfer equations needed to take it account heat losses at the boundary of the bar due to convection and radiation. Taking these losses into account suggest that heat transfer in the z direction should also

be taken into account. This is because if only heat transfer in the radius direction is taken into account then losses out the end of the bar won't be taken into account and only losses out the side towards the coil would be. The radial coordinate can be still assumed to be uniform as the heat generated within the bar is uniform in the radial and z axis.

Since it was identified to add convective and radiation losses as well as heat transfer in the z axis the heat transfer equation needed to be changed to reflect this. The addition of the z axis changes the structure of the nodes from a linear array to a grid with the nodes reflecting positions in the cross section of the bar.

Convection and radiation losses only affect the boundaries of the grid and so different formulas were required for the boundary nodes and interior nodes. Also another formula was required for the corner node as it would experience greater losses than the side nodes.

Currently heat generation was added first and the temperature change was then calculated after and then temperature change due to heat conduction was calculated and added. Instead of this doing this separately for the new model all instances of heat transfer were combined into a single equation. The equations for the interior, side and corner nodes are shown below [8]:

Corner node:

$$\frac{\Delta T_{i,j}}{2F_0} = (T_{i+1,j} - T_{i,j}) + (T_{i,j+1} - T_{i,j}) + 2Bi(TA - T_{i,j}) + H_{i,j} \frac{\Delta x^2}{2k} + 2 \frac{\sigma E \Delta x}{k} (TA^4 - T_{i,j}^4) \quad (13)$$

Side node:

$$\frac{\Delta T_{i,j}}{F_0} = (T_{i+1,j} - T_{i,j}) + (T_{i-1,j} - T_{i,j}) + 2(T_{i,j-1} - T_{i,j}) + 2Bi(TA - T_{i,j}) + H_{i,j} \frac{\Delta x^2}{2k} + 2R(TA^4 - T_{i,j}^4) \quad (14)$$

Interior nodes:

$$\frac{\Delta T_{i,j}}{\Delta t} \frac{\rho_{bar} c_p}{k} = \frac{H_{i,j}}{k} + \frac{T_{i-1,j} + T_{i+1,j} - 2T_{i,j}}{\Delta x^2} + \frac{1}{r} \frac{T_{i+1,j} - T_{i-1,j}}{2\Delta x} + \frac{T_{i,j+1} - T_{i,j-1} - 2T_{i,j}}{\Delta x} \quad (15)$$

The interior nodes are derived directly from the same heat transfer equation shown above (9). The side and corner nodes are as well except that an energy balance is used to account for the losses with the ambient air due to radiation and convection. Analysing the equations also meant there was a new stability criterion that had to be met which is for FO to be less than 0.25.

The plot shows the maximum temperature on the surface of the bar against time for different power settings.

It was noticed that when that over time when the bar started heating up the frequency decreased and the voltage increased where as the current remained the same. This could be due to the resistance increasing in the coil and possibly the cable leads from the ROY increasing in temperature. This would explain the rise in voltage to maintain the same current which would suggest that there isn't a certain power output for a power setting on the ROY but a current setting. This would be more practical for an induction heater as the greater the amplitude of the current the faster the heating in the bar due to a larger magnetic field.

To maintain stability the model will need to calculate the time increment for a set distance between nodes that kept the FO number at 0.25. This is so the maximum time increment is used when doing calculations for a Δx . This again means increasing Δx decreases the time increment but will increase its accuracy.

How the model operated changed as the calculations as the change in temperature due to heat generation and transfer were combined. How the revised model calculates the maximum temperature versus time is shown in figure 4 below.

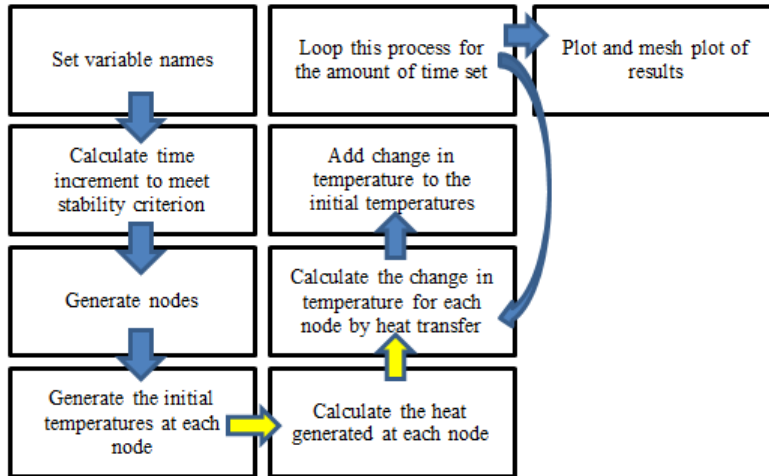


Figure 4. Block diagram outlining how the MATLAB Model works

Yellow arrows are called upon functions and blue are steps in the main script.

The revised model is simpler than the first model as the calculations were combined and with the addition of the z axis more than just a graph of the temperature distribution was produced.

B. Results

When the revised model is finished working it produces three figures and stores the temperatures at each node every 1000 time increments. The first figure is a plot showing the maximum temperature versus time so that it could be compared to the experiments results. The next graph is a 3D mesh plot showing the temperatures at each node in a certain colour depending on how much the temperature was and the last graph is a top view of the 3D

mesh plot. Figure 5 shows the first two figures produced using a current input of 30A, a frequency input of 50kHz and a Δx of 0.00008.

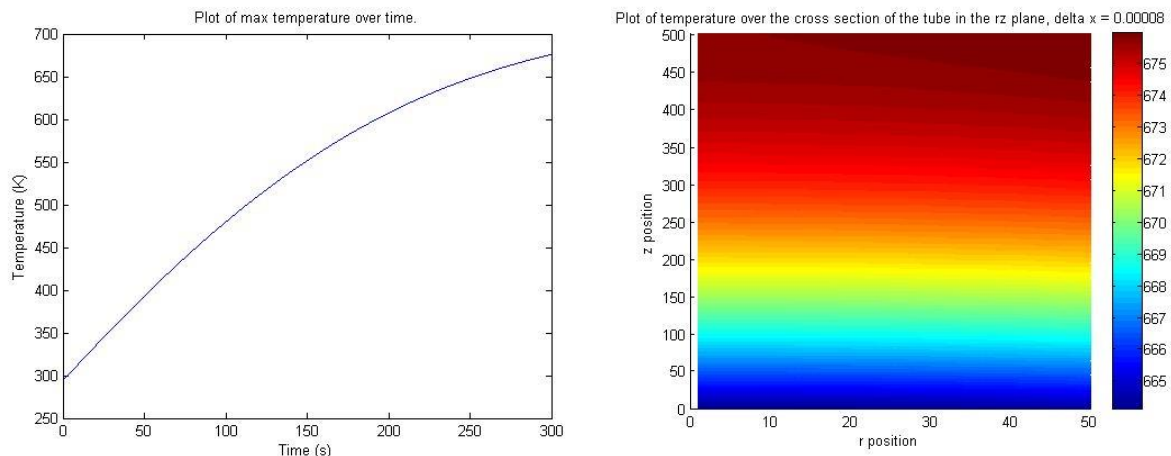


Figure 5. First two figures produced by the revised model

The first figure is the plot of the maximum temperature on the surface against time. The second is the temperature distribution within the bar

When the first figure is compared to the experiments results of a power setting of 5 it shows a similar behavior. If the revised model was to run longer it would show that a finite maximum temperature would be reached. However accuracy of the model can't be achieved without accurate temperature measurements from the experiment. The biggest factor affecting the accuracy of the model is the size of Δx . The second figure suggests that the temperature distribution becomes radially uniform when the maximum temperature on the surface becomes a finite value. This value appears to occur at the top of the bar because the model doesn't take into account the length of the bar outside the coil and so it doesn't have boundary losses at the top. How the temperature distribution changes in the bar with time is shown in appendix A2.

Figure 6 shows that when Δx is decreased the rate of rise in temperature is increased and the point at which the curve starts to reach a finite value occurs earlier as well as reaching a higher finite temperature. If Δx was further decreased the difference in the final maximum temperature between plots should decrease. This would require a more time to run the model as for a Δx value of 0.00008 it had taken four hours to calculate. The

reason for it taking longer to calculate is due to the decrease in the time increment and the increase in the number of nodes.

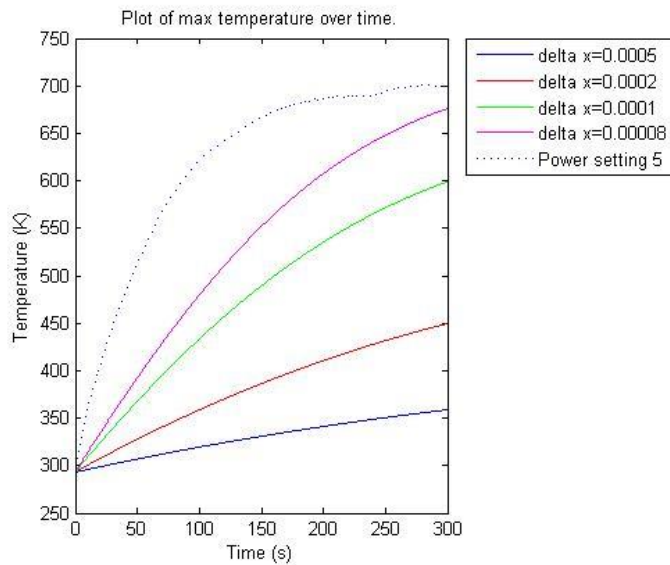


Figure 6. Plots of the maximum temperature on the surface versus time

This figure compares the plots of different Δx values and the results of the experiment with a power setting of 5.

VIII. Conclusions

The aim of this research project was to develop and validate a mathematical model that was able to simulate the heating of a tube by induction. The experiments that were conducted weren't very accurate and so the model wasn't able to be validated. The revised model does however simulate the behavior of the temperature rise within the cross section of a solid round bar. The model can be used to show the temperature rise in the cross section for a desired nozzle configuration and show how changing certain parameters affect the rise in temperature.

IX. Recommendations

Future work on this project would involve validating the MATLAB Model by recording accurate results from an experiment. Once the model has been validated it can be improved to take into account other factors for example the change in properties with rise in temperature. The model can also be reconfigured to model the heating of tube with a depositing metal inside it. This would allow for a nozzle configuration to be tested by simulation and added to the design of a 3D metal printer.

Acknowledgements

I would like to thank Dr Sean O'Byrne for being able to take time out of his schedule to help me with the project.

References

1. Tyagi G., "Introduction to 3D Printing," *3D Printing Technology* [online website], URL: <http://nicsu.up.nic.in/knowdesk/3D-Printing-Technology.pdf> [cited 07 May 2014].
2. McCormack, R., "Proof of Concept for commercial Three Dimensional Extrusion Printer for Metals Using Induction Heating," University of New South Wales, 2013
3. Zinn, S., Semiatin, S.L., *Elements of induction heating: Design, Control and Applications*, ASM International, 1988 Chap 2
4. Walker, J., *Fundamentals of Physics*, 9th ed, John Wiley & Sons, USA, 2011, Chaps. 29, 28, 30, 31
5. Kakac, S., Yener, Y., *Heat Conduction*, 3rd ed, Braun-Brumfield, USA, 1993
6. Unknown, "Heat conduction in Cylindrical and Spherical Coordinates 2," URL: <http://www.ewp.rpi.edu/hartford/~ernesto/S2004/CHT/Notes/s06.pdf> [cited 15 Jul 2014].
7. Unknown, "Table of total emissivity", URL: <http://www.monarchserver.com/TableofEmissivity.pdf> [cited 05 Oct 2014].
8. Croft, D. R., Lilley, D. G., *Heat transfer calculations using finite difference equations*, Applied Science